AN IN DEPTH CHARACTERIZATION OF $(NbTa)_3Sn$ FILAMENTARY SUPERCONDUCTOR

D.P. Hampshire, H. Jones and E.W.J. Mitchell

The University of Oxford, The Clarendon Laboratory, Oxford, OX1 3PU UK.

Abstract

Further to our programme of investigations of new, technical superconductive materials which are of interest to designers of practical devices, we present the results of a detailed study of the critical parameters of the ternary addition A.15 material $(Nb7.5w/oTa)_3Sn$ manufactured by Vacuumschmelze GMBH, Hanau F.R.G. The basis of the results we report is a comprehensive Jc(B, T) characterization within the range, $0<B<15.5T$, $2K<T<Tc$, with particular emphasis on the temperature in the region of Tc. From these data we extract the relevant information relating to the flux pinning behaviour of the material and discuss its implications. The techniques and apparatus used broadly follow those reported previously although some refinements and improvements we have developed will be described.

Introduction

Critical to the development and subsequent utilisation of multifilamentary wire are reliable and reproducible characterizations of their superconducting properties. At the Clarendon, as part of a continuing programme to this end, we have examined a $(NbTa)_3Sn$ conductor[1] consisting of 3721 filaments fabricated by bronze route (bronze: NbTa, 1:2). Using a standard four-terminal technique and a criterion of $10\mu Vm^{-1}$, we have determined the critical current throughout the field and temperature on a 0.4 mm ϕ wire. Using 0.7 mm ϕ wires we have compared this ternary intermetallic compound with its parent Nb_3Sn and confirmed its higher critical current at $B \gtrsim 10T$, $T < 4.2K$, in agreement with the manufacturers published data.

Experimental Procedure

Sample Mounting

The wire is helically wound on a cylindrical sample holder grooved with a 3 mm pitch. The sample holder consists of two thick-walled O.F.H.C. copper tubes. These are shrink-fitted into thin-walled stainless steel and kept mechanically discontinuous by a thin layer of ceramic (as shown in figure 1). The sample holder is designed to provide maximum thermal conductance, whilst retaining the integrity of the stainless steel which acts as a parallel electrical shunt to the sample. Following reaction (10^{-5}Torr at 973 K for 64 hours), the wire was soldered directly to the sample holder following broadly a technique described elsewhere.[2†] Finally, potential taps were soldered 300 mm along the sample length, symetrically about the field centre.

The Variable Temperature Probe

The operation of this probe has been extensively detailed elsewhere.[3] Essentially, the sample holder is clamped between two copper electrodes beneath which lies a bifilar concentrically wound heater. Temperature measurement and control is achieved by three thermometers - a Rh-Fe standard and a field independent strontium titanate capacitance thermometer (Lakeshore CS400) in the upper electrode, with a calibrated carbon glass in the lower electrode. The sample holder and heater assembly are enclosed in a quasi-isolated thermal enclosure, the construction of which is summarised in figure 2. Previously, electrical contact to the sample holder was via indium coated demountable clamped contacts. These soft surface coatings were believed to give the lowest interface resistances. However, as a result of the limited clamping force that can be achieved with this probe, significant Joule heat was produced at these joints in high current. However, we achieved at least an order of magnitude reduction in the joint resistances by using Wood's Metal as a solder. As a result of the low melting point of Wood's Metal, we were able to apply an external clamping force (at $T \leq 85^oC$) to these contacts while the surfaces were still molten. Nevertheless, once the external clamp is removed, owing to the comparative lack of mechanical strength of this type of joint, it is essential the probe is not strained or shocked.

Measurements

For $T \geq 4.2$ K, before each set of measurements the capacitance thermometer was calibrated in zero field using the Rh-Fe thermometer. The temperature was then kept constant by using this field-independent capacitance control thermometer in closed loop with the heater winding via a Lakeshore Bridge. At $T \leq 4.2$ K, the brass jacket was removed and the sample was immersed directly in liquid helium. The temperature was determined by vapour pressure control, and stabilized by monitoring a manometer connected by a static line to the pumped dewar. The temperature difference between the top electrode and the bottom electrode was determined as a function of sample temperature - defined by the Rh-Fe in the upper electrode. $|\Delta T(T)|$ was found to be $\leq 0.5^oK$ throughout the temperature range. At each field and temperature, the sample current was ramped up at $\leq 5A.s^{-1}$ and a V-I characteristic generated.

Accuracy

The magnet used for the 0.4 mm ϕ wire test was the Oxford Hybrid Magnet. For the 0.7 mm ϕ wire our Jc(B)[3] probes were used in conjunction with our 16T superconducting magnet. Our quoted field values are accurate to $3x10^{-3}$ Tesla - determined using n.m.r. techniques. Sample current was measured using a shunt of accuracy $< \pm 1\%$. The greatest source of inaccuracy is due to possible temperature gradients between our thermometers and the sample wire. In an effort to quantify experimentally the accuracy of our results, we attempted mounting a small calibrated diode thermometer close to the relevant wire windings within the voltage taps. Unfortunately because of limited space within the isolated enclosures, thermal contact between the sample wire and the thermometer could not be guaranteed. However we

†Unfortunately during the period between the completion of the measurements above 4.2°K and commencing those for 4.2°K and below, our first sample was damaged - corrosion due to trapped acidic flux and simple mechanical damage are two possible candidates. Hence our results for 4.2°K and below are for a second sample. The results from the two samples are wholly compatible.

Manuscript received September 10, 1984

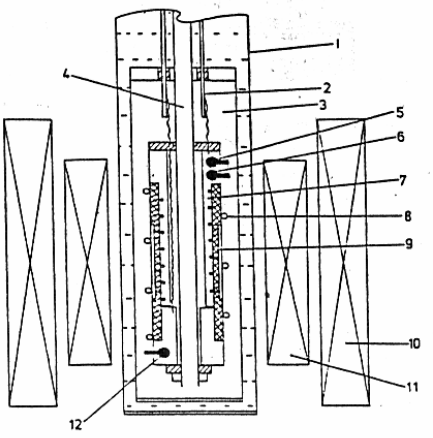

Fig.1-2

1. Dewar tail
2. High current lead-throughs
3. Vacuum tight enclosure
4. Pumping tube
5. Rh Fe reference thermometer
6. Capacitance control thermometer
7. Copper heater block and heater
8. Helically wound sample
9. Copper and stainless steel sample holder
10. Hybrid magnet superconducting outer section
11. Hybrid magnet resistive inner section
12. Lower carbon glass resistance thermometer

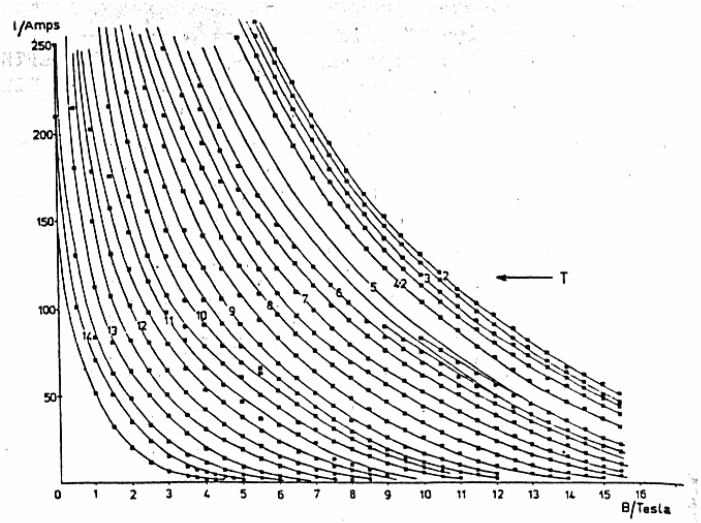

Fig.3 Critical Current vs Field As A Function Of Temperature For $(NbTa)_3Sn$

expect the inaccuracy in the temperatures we have given to be similar to that found in previous work. Having assumed a linear gradient, this was quoted at ± 0.25°K.

Results

A detailed micrographic investigation of the 0.4 mm ϕ wire suggests the filaments are ≥ (90%) reacted. Hence our quoted overall current densities can be increased by a factor of ∿ 3/2 to find the current density in the superconducting layer. The data collated for the 0.4 mm ϕ wire are shown in figure 3. Only low current data points can be obtained at 5 K and 5.5 K, since at higher currents the closed loop heater control cannot combat the Joule heat. The enhanced critical current of this material in high fields is explicitly demonstrated when a comparison is made between 0.7 mm ϕ Nb_3Sn and 0.7 mm ϕ $(NbTa)_3Sn$. This is shown in figure 4 in which $(\text{current})^{\frac{1}{2}}(\text{field})^{\frac{1}{4}}$ vs (field) is plotted as a function of temperature. It has been suggested[5] that the Ta may effect a more stabilised A15 structure or perhaps a change in electronic structure. If this occurs at the expense of a decrease in the strength of the pinning sites, it would certainly account for the cross-over at 10T. These data suggest that, in principle at least, it should be possible to achieve a 20 Tesla magnet operating below the lambda point in this material.

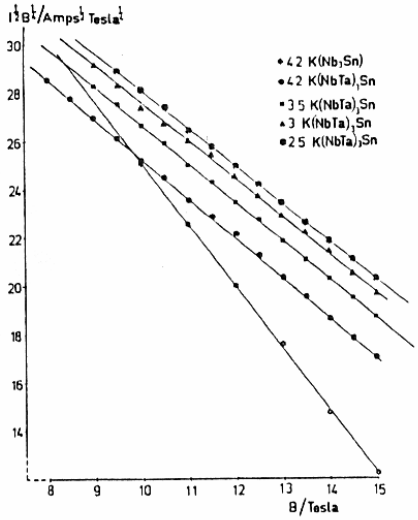

Fig.4 A Plot Of $(I^{\frac{1}{2}}B^{\frac{1}{4}})$ vs B For Nb_3Sn And $(NbTa)_3Sn$ (0.7mmϕ) As A Function Of Feild

T ≳ Tc

In order to determine the extent of inhomogeneity in the material, resistive and inductive Tc measurements were made. For a sample current of 0.25A: Tc(Res) = 16.5K [10% 16.1K, 90% 17.0K]. In zero field, Tc(Ind) = 15.9K [10% 13.7K, 90% 17.1K]. These results are in agreement with the extrapolation of our data which suggests: $Tc(B_{c2}=0) = 16.8K \pm 0.5K$. The width of the transitions which we have observed are typical for A-15 systems of this type. They can be attributed to a long range variation in Tc.

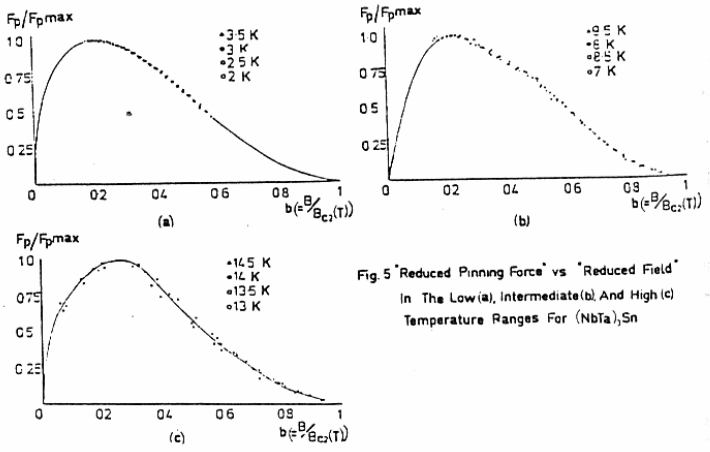

Fig.5 "Reduced Pinning Force" vs "Reduced Field" In The Low (a), Intermediate (b) And High (c) Temperature Ranges For $(NbTa)_3Sn$

Flux Pinning and Scaling Laws

In addition to the technological data, this analysis gives fundamental information about the flux pinning mechanisms which control J_c. As has been documented for other A15 materials,[6] by considering figure 5, we can see to a first approximation a Scaling Law holds. We now discuss the field and temperature dependence of this Scaling Law.

Field Dependence

In figure 6 we have re-analysed the data in figure 3 plotting $(\text{current})^{\frac{1}{2}}(\text{field})^{\frac{1}{4}}$ versus (field) as a function of temperature. Throughout the entire temperature range we find a first-order linear dependence. It is clear that any theoretical model must give:

$$F_p \propto h^{\frac{1}{2}}(1-h)^2 \text{ where } h = (H/H_{c2}) \qquad (1)$$

We now briefly consider each of two fundamentally different, well established, pinning models which give the required dependence in the high-field limit ($h \gtrsim 1$):

i) Kramer's Flux-Shear Model

Kramer's model[6] considers regions wherein fluxons are held fixed by planar pins. When the critical current is reached, unpinned fluxons which experience the electrodynamic force, shear past these regions. As a result of this motion the unpinned fluxons experience dissapative distortions which generate a voltage. By considering the flux-line-lattice Kramer found:

$$F_K = \frac{P}{(1-A_o\sqrt{\rho})^2} H^{\frac{1}{2}} H_{c2}^{\frac{1}{2}} C_{66} \qquad (2)$$

P: constant prefactor; A_o: interflux-line spacing; H_{c2}: upper critical field; ρ: density of pinning sites; C_{66}: elastic constant.

In the limit $1-h \ll 1$, Labusch[7] has shown:

$$C_{66} = 0.1\ \mu_o \left[\frac{H_{c2}(T)}{K(T)}\right]^2 (1-h)^2 \qquad (3)$$

which gives the required high field dependence for $F_K(B,T)$. However in intermediate fields ($H_{c1} \ll H \leq H_{c2}$), one must consider the full-non-linearised Ginzburg-Landau equations. Within this framework Brandt[10] has shown that to a good approximation:

$$C_{66} = \mu_o H_c^2(T)\ \frac{b(1-b)^2}{4}\ (1-0.29b)\ \exp\left(\frac{b-1}{3K^2 b}\right)\ f(K) \qquad (4)$$

where f(K) is a function of the Ginzburg-Landau constant K, and $b \approx h$ for large K. This full interpolation for C_{66} shows significant deviation from the expression for the high field limit for all K, and $h > 0.4$. This incompatability between the Kramer model and our data in low fields (demonstrated in fig 7 for K = 10) undermines the probability of shearing being the critical pinning mechanism close to H_{c2}. Only a conspiratorial relation between flux pinning and flux shearing would explain the linearity in our data throughout the field range - this we consider unlikely.

ii) Dew-Hughes[9] core pinning model

By considering the core pinning of fluxons by planar regions of normal material, Dew-Hughes found an expression for the bulk pinning force of the form:

$$F_D = (Sv/1.07)(B/\phi_o)^{\frac{1}{2}}\ \pi\xi G \qquad (5)$$

where Sv is the surface area properly orientated to be effective in pinning. ξ the coherence length and G the [illegible]e energy.

We now consider this expression in all but the lowest fields. By substituting Brandt's[8] general solution for the free energy, we find:

$$F_D \propto \frac{\mu_o H_{c2}^2}{K^2}\left[\bar{h}^{\frac{1}{2}}(1-h)^2 + 2.32\bar{A}\ \exp - \bar{B}h\right] \qquad (6)$$

for K = 10 $\bar{A} = 0.036$ $\bar{B} = 7.35$. ($H_{c1} \ll H < H_{c2}$).

This predicts a linear relation between (current)$^{\frac{1}{2}}$ (field)$^{\frac{1}{4}}$ and (field) to within 2% at each temperature in intermediate and high fields. Thus it agrees with the field independence of our data to within the experimental accuracy.

Temperature Dependence

The straight lines in figure 6 certainly suggest a unique $H_{c2}(T)$ can be associated with each temperature. Using a computerised least-squares straight-line-fit, we have determined $H_{c2}(T, I=0)$. This is plotted in figure 8. It is interesting to note that $H_{c2}(3^oK) \approx$

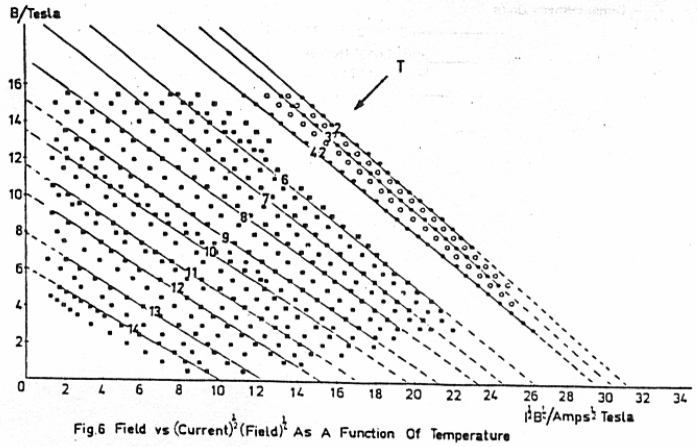

Fig.6 Field vs (Current)$^{\frac{1}{2}}$(Field)$^{\frac{1}{4}}$ As A Function Of Temperature

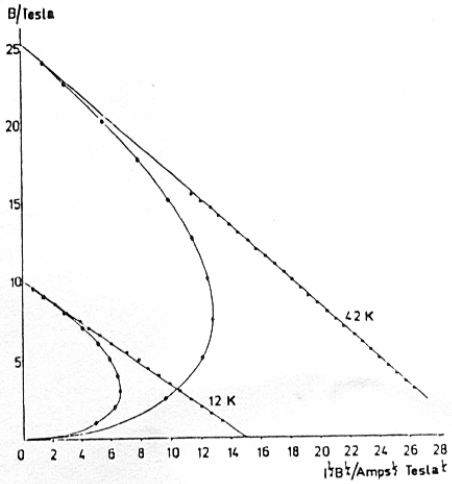

Fig.7 A Comparison Between F_K And The Experimental Results For $(NbTa)_3Sn$ At 12 K And 4.2 K

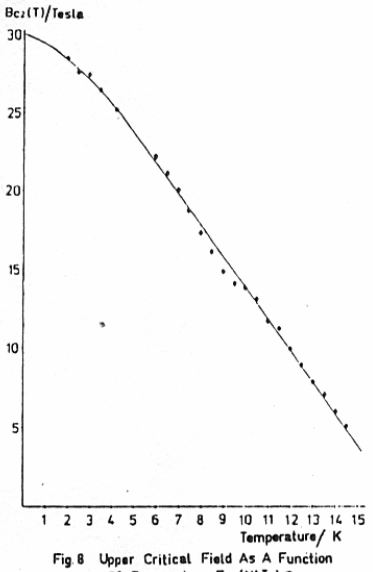

Fig.8 Upper Critical Field As A Function Of Temperature For $(NbTa)_3Sn$

$H_{c2}(2.5^oK)$ for both the 0.7 mm ϕ wire and the 0.4 ϕ wire. The determination of H_{c2} in each case was completely independent - a different set of magnet, pumps, and temperature monitoring systems was used in each case. We feel this temperature independence is a function of the inhomogeneity of the material and the way in which this extrapolated $H_{c2}(T)$ is defined (i.e. $H_{c2}(T) = H_{c2}(T, I=0)$).

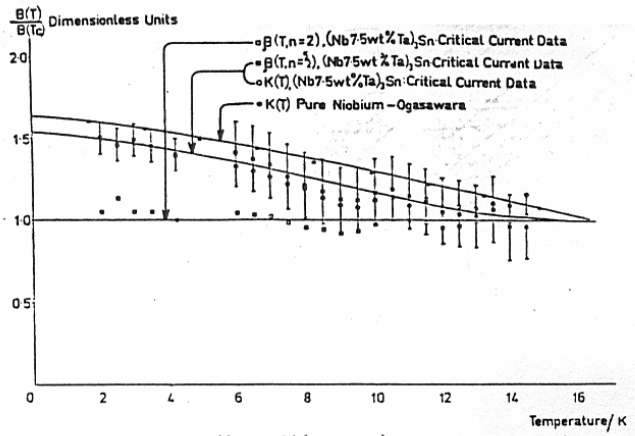

Fig.9 A Comparison Between B(T) And K(T) (Normalised) As A Function Of Temperature

Consider the general equation:

$$Fp = \frac{H_{c2}^{n}(T)}{\beta^{2}(T)} h^{\frac{1}{2}}(1-h)^{2} \qquad \alpha,n: \text{ constants} \quad \beta(T) = f(K(T)) \qquad (7)$$

If we use an empirical relation[5] between $H_{c2}(T)/Tc$ and K(T) of the form:

$$H_{c2}(T)/Tc = \gamma(1-\tau^{2})\ K\ (T) \qquad \gamma: \text{ constant} \quad \tau = T/Tc \qquad (8)$$

we can solve for K(T). In figure 9, we have compared $K(T)/K(Tc)$, derived from equation 7, with $\beta(T)/\beta(Tc)$ for n = 2 (normalized at Tc) and n = 5/2, (normalised at T = 4.2°K) determined from equation 8 using our critical current data.

For n = 2 we find $\beta(T) \approx$ constant, therefore:

$$F(H,T) \approx \phi H_{c2}^{2}(T)\ h^{\frac{1}{2}}(1-h)^{\frac{1}{2}} \qquad \phi: \text{ constant} \qquad (9)$$

although this predicts $\log F_{pMAX}(T) = 2 \log H_{c2}(T)$ + constant, we consider this law of limited significance since we find no K(T) dependence. This in our opinion calls into question the Dew-Hughes model. For n = 5/2 to a good approximation $\beta(T) \approx K(T)$ hence:

$$Fp = CH_{c2}^{5/2}(T)\ h^{\frac{1}{2}}(1-h)^{2}/K^{2}(T). \qquad C: \text{ constant} \qquad (10)$$

where the next correction term to this empirical formula requires only a different temperature dependence.

Although our magnetization Tc experiments suggest a long-range variation in Tc and significant inhomogeneity, our critical current data suggest a unique and characteristic $H_{c2}(T)$ and K(T). An interesting facet of our data is the strong temperature dependence of K(T). Consideration of $K_{empirical}$ suggests this is an intrinsic feature of the material in the region of pinning, and does not indicate the need to insert an additional temperature dependent pinning strength function $\phi(T)$. Furthermore, introducing $\phi(T)$ would tend to lessen the good equivalence we have found between $\beta(T)$ and K(T) (i.e. $\beta(T) = K(T) \neq f(K(T), \phi(T))$). Large values of $K(0)/K(Tc)$ have been observed previously. In figure 9 a magnetization measurement[11] for $K(T)/K(Tc)$ for pure niobium can be compared with our data. Nevertheless, we expect our good correlation between $K_{empirical}(T)$ and K(T, n = 5/2) to breakdown for T > 13.5K, as a result of localised, low Tc regions going normal, a redistribution of current in the filaments and the region in which critical pinning occurs changing. We are at present considering a programme wherein we gather more data in the critical range $T_{c1} < T < T_{c2}$.

It has been suggested that in order to present a satisfactory explanation of our data and the anomalous variations in temperature found experimentally in some pure materials, a greater consideration of the anisotropy of the Fermi surface and the many-body electron-electron interactions (and their associated spin fluctuations) will be necessary. Evidently a full understanding of the scattering processes and hence pinning in this inhomogeneous intermetallic compound is a formidable task.

Conclusion

In this paper we have presented a detailed study of the critical current of $(NbTa)_3Sn$. Our results demonstrate the higher critical currents of this wire over Nb_3Sn for superconducting windings in high fields. We have found an empirical relation giving Jc(H,T) in terms of critical parameters:

$$Jc = \alpha \frac{H_{c2}^{3/2} h^{-1/2}(1-h)^{2}}{(K(T)/K(Tc))^{2}} = \alpha'(\mu_o H_{c2})^{-1/2}(1-\tau^{2})^{2} h^{-1/2}(1-h)^{2} \qquad (11)$$

where $\tau = T/Tc$; $h = H/H_{c2}(T)$; K(T) is determined in the region of pinning; $Jc/Amps.cm^{-2}$; α' (Jc overall) = $8\times10^{4}/A.cm^{-2}.T^{1/2}$ ($\pm$ 3%T $\leq$ 4.2 K, $\pm$ 12% 6 K<T<T_{c1}).

However we have, as yet, found no satisfactory model for the critical current in this A15 material.

Acknowledgements

The authors wish to thank: Alan Day for his help with the presentation of this paper, and Martin Whitworth, who helped with the operation of the hybrid magnet. We are indebted to Y. Hasiscek for his very informative micrographs, P. Upahdyay for the inductive Tc measurements, J. Singleton for the N.M.R. calibrations, Peter Hirst and Jack Day. One of the authors (D.P.H.) is indebted to the S.E.R.C. and Oxford Instruments Co. for financial support.

We would also like to pay tribute to the late P.A. Hudson who initiated many of the facilities described in this paper.

References

1) E. Springer, M. Wilhelm, H.J. Weisse, G. Rupp. "Properties of $(NbTa)_3Sn$ - Filamentary Conductors". CX-8 ICMC (1983).
2) H. Jones, P.A. Hudson, Y.S. Hascicek, S. Nourbaksh, M.J. Goringe. "The Mounting of Samples of Filamentary A15 Superconductor for Jc tests". Cryogenics p 557 (1983).
3) P.A. Hudson, F.C. Yin and H. Jones. The critical current of Nb_3Sn. IEEE MAG 19 (1983).
4) P.A. Hudson, H. Jones, H.M. Whitworth. Centralised High Field Facilities at Oxford. J. de Physique. Proc. MT 8. (1983).
5) M. Suenaga. Superconductor Materials Science. Plenum Press. p 268/252 (1981).
6) E.J. Kramer. Scaling Laws for Flux Pinning in Hard Superconductors. J. App. Phys. 41, 421 (1970).
7) R. Labusch. Elastic Constants of the Fluxoid Lattice near the Upper Critical Field. Phys. Stat. Sol. 32. 439. (1969).
8) E. Brandt. G-L Theory of the Vortex Lattice in Type II Superconductors for all values of K and B. Phys. Stat. Sol. B 81, 345, (1972).
9) D. Dew-Hughes. Flux Pinning Mechanisms in Type II Superconductors. Phil. Mag. 30, 293, (1974).
10) E. Brandt. On the Shear Modulus of the Flux-Line Lattice. Phys. Stat. Sol. B 77, 551 (1976).
11) T. Ogasawara, Y. Kubota, K. Yasukochi. Magnetic Properties of Superconducting Niobium-Tantalum Alloys. J. Phys. Soc. Japan 25, 5, (1968).